

AN AERODYNAMIC PERSPECTIVE ON IMPACTOR API SOURCES

Steve Bajic
Waters Corporation, Altrincham Rd, Wilmslow, SK9 4AX, UK

INTRODUCTION

Electrospray ionisation (ESI), when conducted at low flow rates (10-1000nL/min) is known to be a highly efficient ionisation mechanism. However, high-flow rate ESI, as utilised at LC or UPLC flow rates (0.1-1.0mL/min), is highly inefficient. Ionisation efficiency is critically dependent on a number of factors such as droplet size distribution, droplet charge per unit volume, droplet evaporation rates and additional factors such as the inlet sampling efficiency. Here, we describe an Impactor API source which attempts to increase ionisation efficiency at high flow rates by interacting a high velocity spray with a high voltage, cylindrical target that is positioned in an off-axis, cross-flow arrangement. A number of physical processes will be described which are believed to be important mechanisms that lead to enhanced Impactor source sensitivity when compared to ESI, viz. high Weber number droplet impacts, the Coanda effect, vortex shedding and counter-rotating surface microvortices.

WHAT IS AN IMPACTOR API SOURCE?

An Impactor API source is shown schematically in Figure 1. The spray from a nitrogen-assisted, grounded, concentric nebuliser is directed at one side of a Ø1.6mm cylindrical, stainless steel target that is held at typically 1-4kV and is upstream of the ion inlet of the mass spectrometer. The distance between the nebuliser and the impactor target is kept small so that the near supersonic nitrogen jet impinges directly

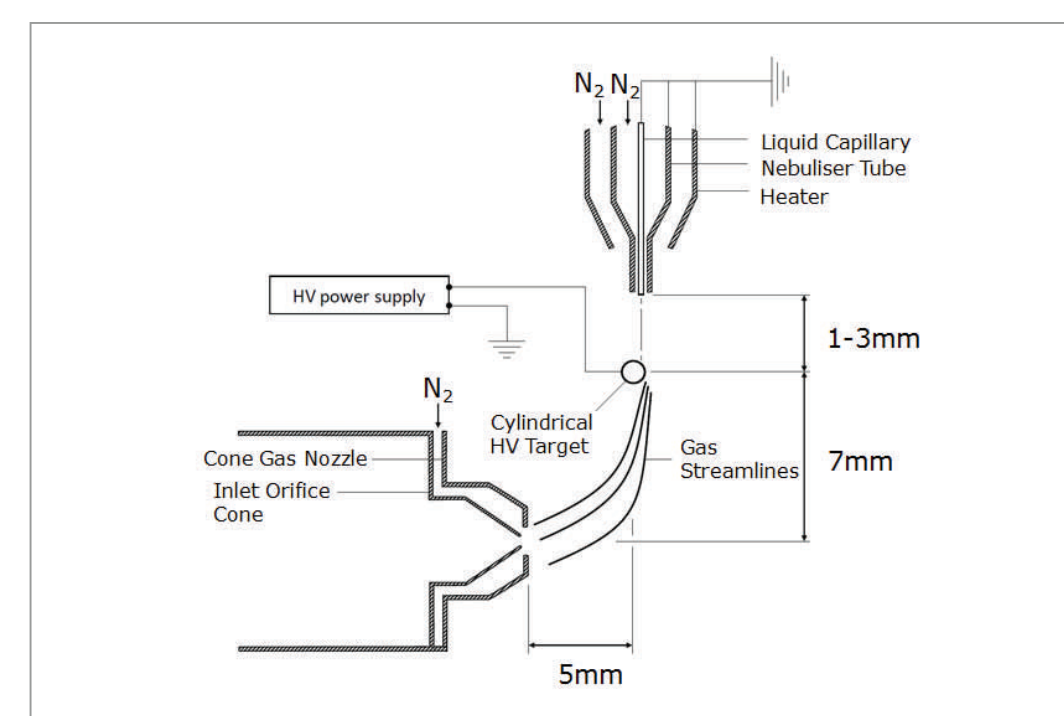


Figure 1. A schematic of an Impactor API source.

on the surface. The off-axis, cross-flow geometry results in the gas flow becoming attached to the target surface such that the wake is directed towards the ion inlet of the MS (Coanda Effect). For most analytes, Impactor sources give rise to mass spectra that are qualitatively equivalent to ESI. However, Impactor sources are known to produce greater ion signals where the enhancement factor over ESI generally increases with increasing aqueous content and increasing pH. The Waters UniSpray source is a commercially-available example of this type of API technology.

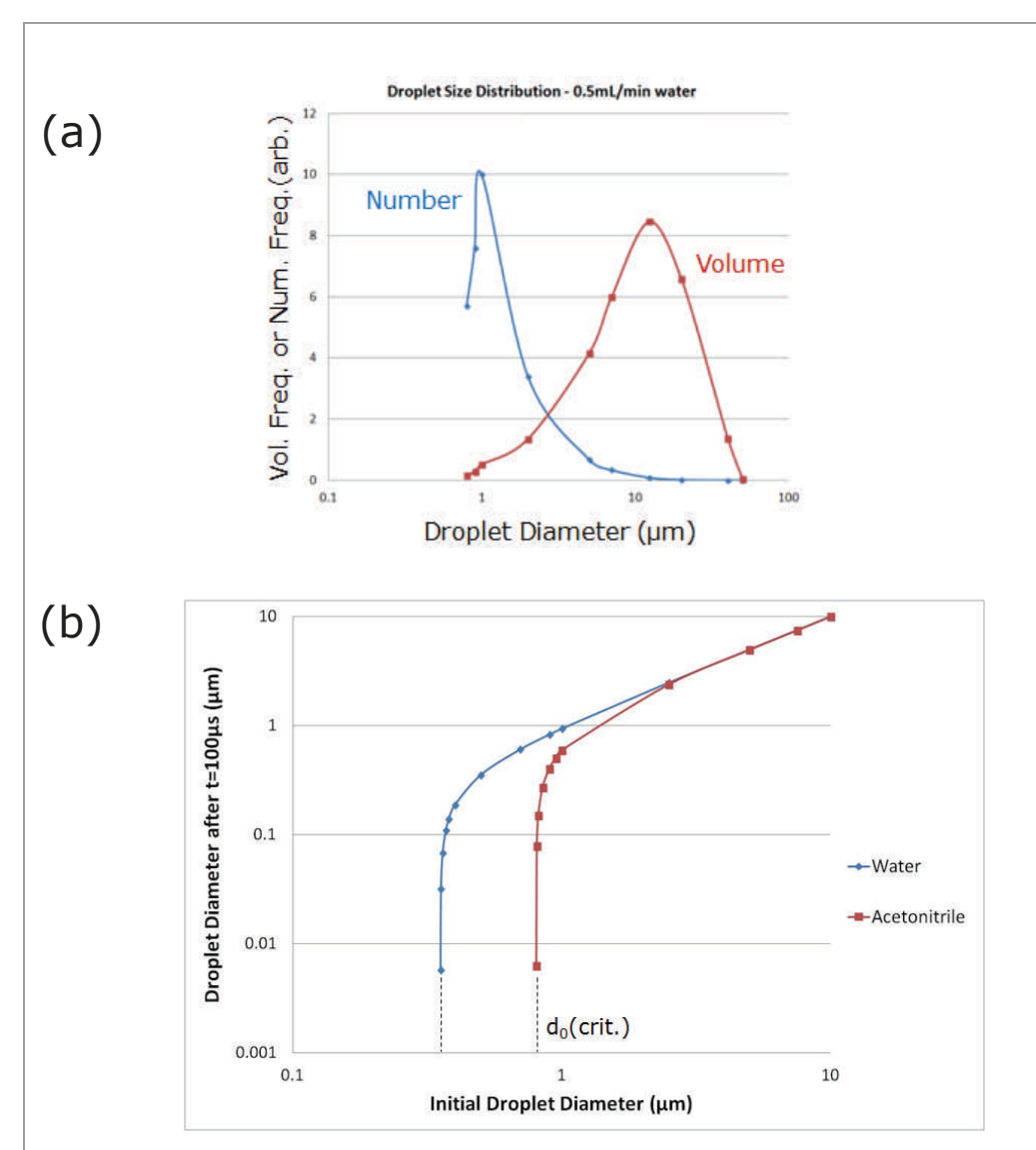


Figure 2. (a) ESI Droplet size distributions for 0.5mL/min of water. (b) Droplet evaporation rates for water and acetonitrile.

RESULTS AND DISCUSSION

Limitations of High Flow Rate ESI

In the traditional ESI model, charged droplets are formed by double-layer charge separation in the high electric field region at the tip of the liquid capillary. At nano flow rates (<1µL/min), this process proceeds with extremely high efficiency to yield highly-charged, sub-micron droplets that almost instantaneously give rise to gas phase ions due to Rayleigh disintegration processes. However, at high flow rates (0.1-1.0mL/min), it is necessary to aid the nebulisation process by the use of a high velocity nitrogen stream. This produces larger droplets than obtained at nano flow rates where the high gas velocity results in droplet velocities that can exceed 120m/s. At these velocities, droplets typically have a source

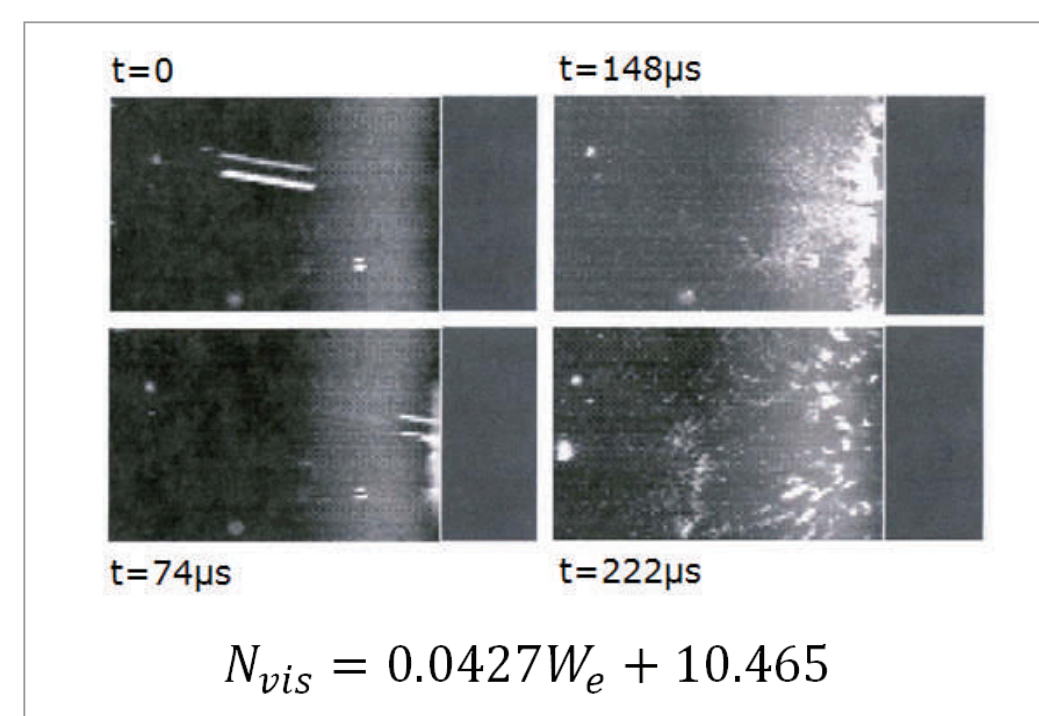


Figure 3. Time lapse photograph of the break-up of a water droplet ($W_e=630$) on a hot metal surface (from [2]).

residence time of 100µs (between the sprayer and the ion inlet) where droplet evaporation must occur. Figure 2(a) shows a typical droplet size distribution for high flow ESI which was obtained by a LDPS analyser (Malvern Instruments, UK). Here, it is shown that although the droplet number distribution peaks at diameters of 1µm, the overwhelming volume of the spray is contained within droplets between 2 and 50µm in diameter. Figure 2(b) shows the relationship between initial and final droplet diameter for a 100µs evaporation time, obtained from parameters determined by the ping-pong drift tube method [1]. This relationship shows that significant evaporation only occurs at initial diameters that are below the "knee" of the curve, which corresponds to diameters of approximately 1.0 and 0.4µm for acetonitrile and water, respectively. Furthermore, Figure 2(a) suggests that the sub-micron droplet population accounts for less than 1% of the high-flow rate water distribution which could account for the low ionisation efficiency of high-flow ESI versus nanospray ESI.

High Weber Number Droplet Impacts

The evaporation rate limit described above was the original inspiration for an Impactor-type source where relatively large droplets are reduced in size via high-momentum impacts with

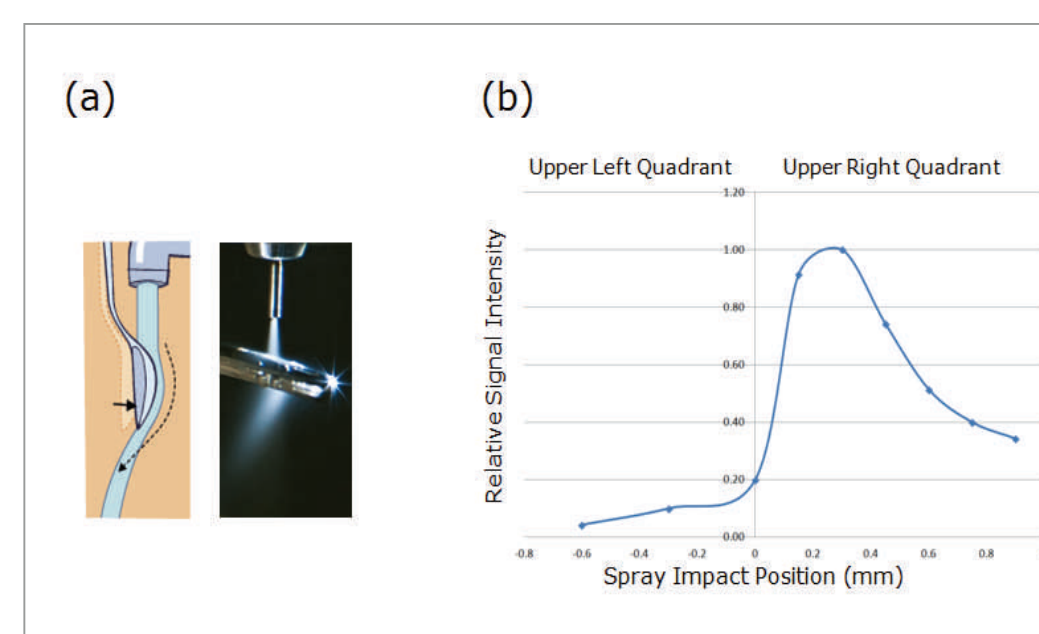


Figure 4. (a) A demonstration of Coanda flow at the impactor target. (b) Dependence of ion signal on point of impact.

a solid surface. The disintegration of water droplets on hot metal surfaces has been studied in detail [2]. It is found that the number of visible secondary droplets (N_{vis}) is directly proportional to the Weber number (W_e) of the droplet (Figure 3) which is given by

$$W_e = \rho v^2 d / \sigma$$

where ρ is the liquid density, v is the droplet velocity, d is the diameter and σ is the surface tension. Thus, a water droplet with a diameter of 4µm and a velocity of 100m/s would have a Weber number of 571 that would give rise to 35 visible secondary droplets on impact. Considering a simple, linear break-up model, this would result in secondary droplets with diameters of the order 1.2µm. More realistically, a skewed Gaussian distribution for the secondary population would contain sub-micron droplets that could evaporate in a 100µs source residence time.

The Coanda Effect—Vortex Shedding

The Coanda effect is a phenomenon whereby a gas flow attaches itself to a convex surface and is shown schematically in Figure 6(a). Figure 4 (a) and (b) demonstrate the effect as it applies to the nebuliser jet flow around a Ø1.6mm impactor target. The effects of "beam steering" are shown in Figure 4 (b). Here, an optimum is reached as the spray impinges on

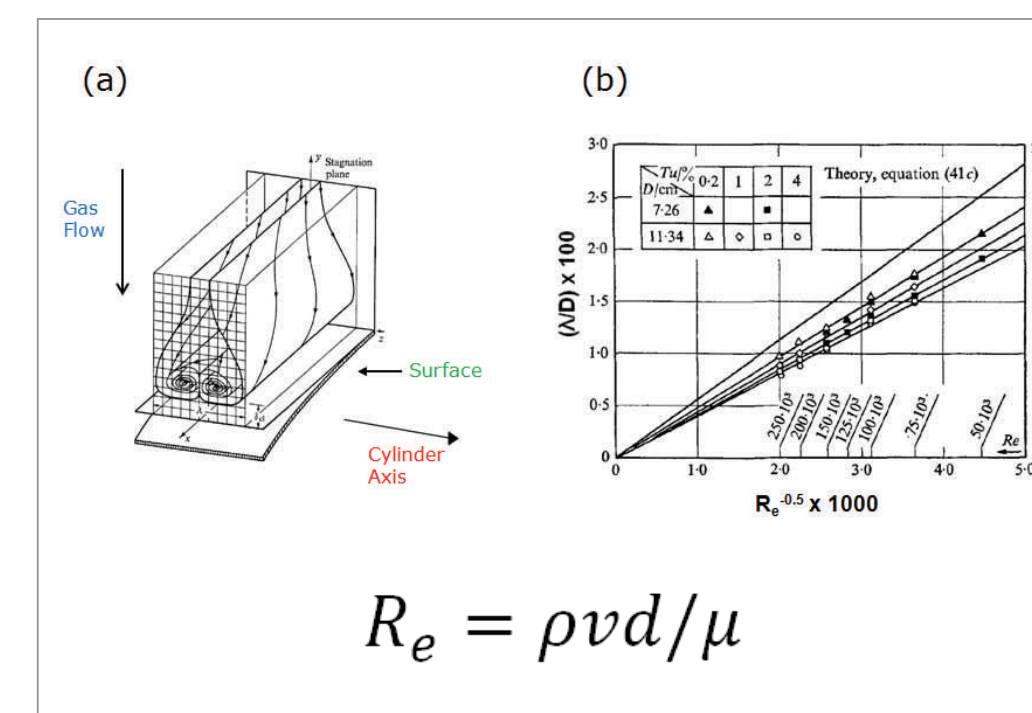


Figure 5. (a) A schematic representation of a single, counter-rotating, surface vortex pair. (b) Experimentally determined relationship between λ and Reynolds number (Re). From [3].

the right hand quadrant of the cylindrical target. Impacting on the upper left hand quadrant of the target results in a severe loss of ion signal as the deflected wake is directed away from the ion inlet cone and ion sampling efficiency is adversely affected. The Coanda effect could also enhance the desolvation of droplets by (i) increased nitrogen gas entrainment when compared to an "open" geometry and (ii) turbulent mixing in the vortex shedding region of the wake flow. The vortex shedding frequency (f_s) is known to increase with increasing flow velocity and is given by

$$f_s = S_r v / d$$

where v is the freestream flow velocity, d is the target diameter and S_r is the dimensionless Strouhal number.

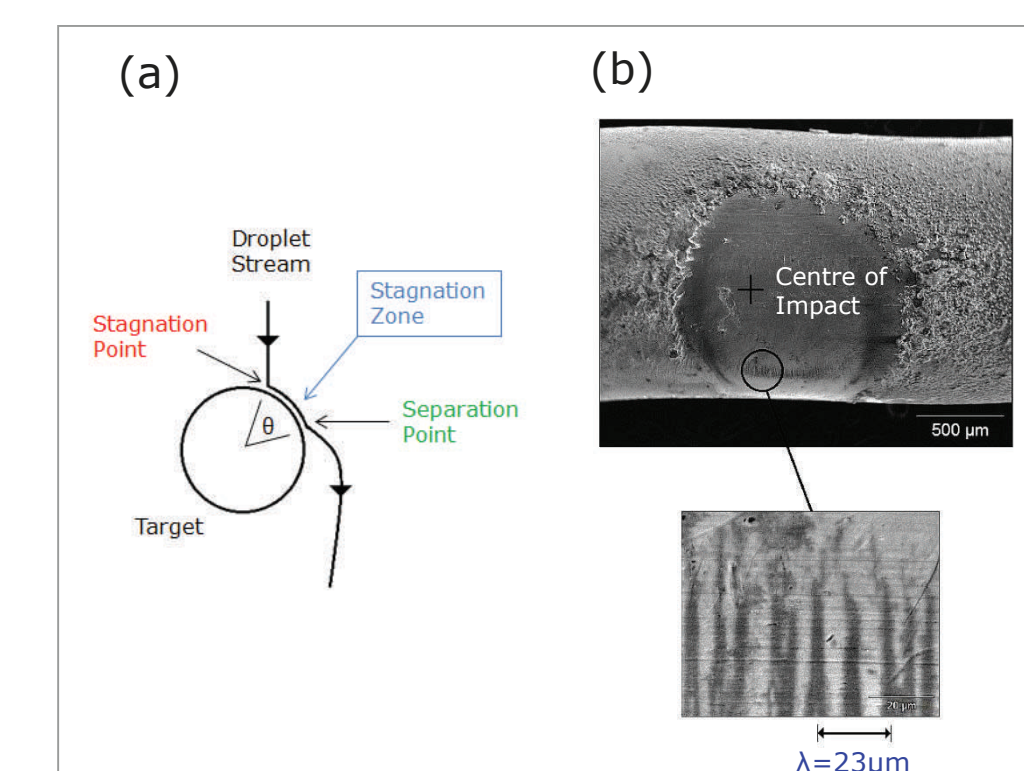


Figure 6. (a) A schematic of the flow stagnation zone that exists at the impactor target surface. (b) SEM micrograph of striation marks on a Ø1.6mm impactor target.

For a near-supersonic nitrogen gas flow ($v=300\text{ms}^{-1}$) and a Ø1.6mm cylinder, it can be shown that S_r is approximately equal to 0.2 and the vortex shedding frequency (f_s) in the wake of the impactor target will be typically 37kHz, i.e. ultrasonic.

Cross-flow Surface Microvortices

At the near supersonic jet velocities encountered in Impactor API sources ($v=300\text{m/s}$, $Re=30,000$), the flow stagnation zone (Figure 6(a)) can be shown to have a radial thickness of the order of 10µm, over which a flow velocity gradient exists from zero at the surface up to the freestream velocity (v). Primary or secondary droplets that enter this reduced velocity region would be expected to experience enhanced desolvation due to (i) an increased residence time, (ii) greater thermal transfer from the hot target surface and (iii) increased agitation/mixing with the hot nitrogen flow due to surface vortex effects.

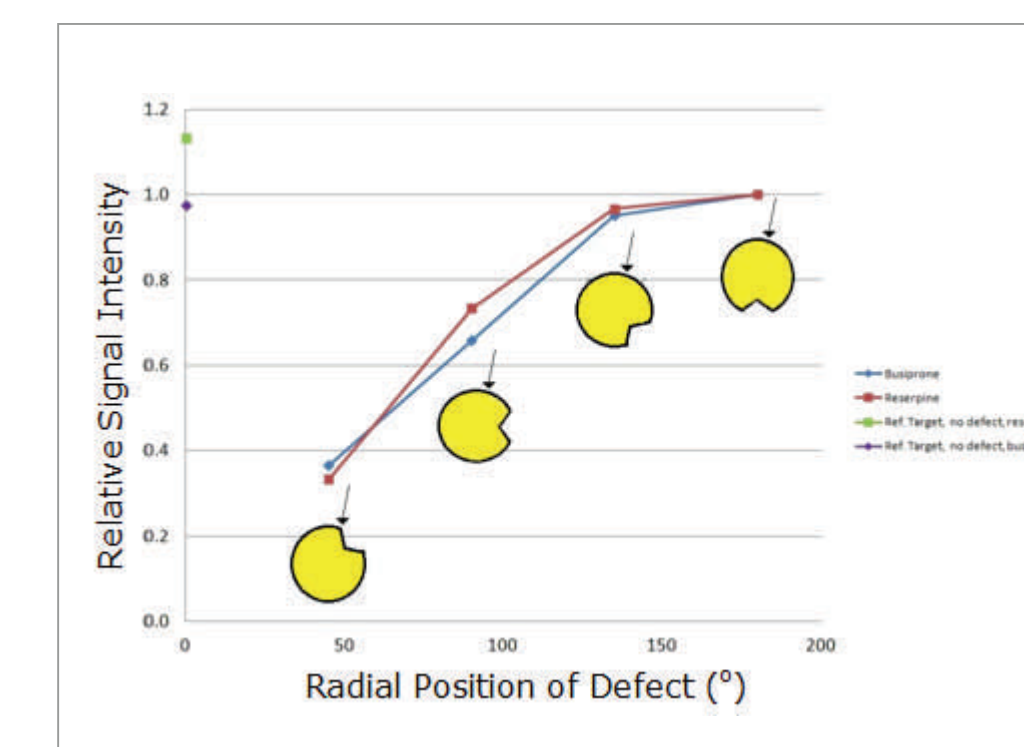


Figure 7. How the radial position of a circumferential defect on the Ø1.6mm target can adversely affect ion signal. The arrow denotes the spray impact point.

Surface vortex effects are unique to cross-flow over a curved surface and have been studied in detail [3]. These vortices in the stagnation zone manifest as a linear series of counter-rotating vortices whose axes of rotation are aligned with the streamlines of the gas flow. A schematic of a counter-rotating pair is shown in Figure 5(a). The disturbance wavelength, λ , between adjacent counter-rotating pairs is given by

$$\lambda = \kappa d / \sqrt{Re}$$

where κ is a constant and d is the target diameter. For near supersonic flow on a Ø1.6mm target, the experimental data of Figure 5(b) would predict a disturbance wavelength (λ) of 37µm. In support of the existence of surface microvortices under these conditions, Figure 6(b) shows a SEM micrograph of a used Impactor source target. Here, a series of striation marks with a value of $\lambda=23\mu\text{m}$ is clearly visible.

Finally, it should be made clear that Impactor source enhancements over ESI are not observed with flat plate targets. To reinforce the importance of the stagnation zone effects described above, Figure 7 shows how Impactor source sensitivity is adversely affected by adding a surface defect to a Ø1.6mm target where the defect is approximately equivalent to the circumferential size of the stagnation zone ($\theta=46^\circ$). Here, the highest signal intensity is observed when the defect cannot influence the stagnation zone (upper right hand quadrant) and vice versa.

CONCLUSION

- An Impactor API source has been described that can give rise to enhanced sensitivity when compared to high flow rate ESI
- It is postulated that the effects of droplet impactation, Coanda steering, vortex shedding and surface microvorticity can enhance ionisation efficiency
- In particular, it is believed that the enhanced ionisation efficiency is related to the flow of gas around curved surfaces.

References

- [1] R.L. Grimm and J.L. Beauchamp, Anal. Chem. **74**, 6291-6297 (2002)
- [2] S.W. Akhtar, G.G. Nasr and A.J. Yule, Atomisation and Sprays, **17**, 659-681 (2007)
- [3] J. Kestin and R.T. Wood, J. Fluid Mech., **44**, 461-479 (1970)